Available online at www.sciencedirect.com

ScienceDirect

Geochimica et Cosmochimica Acta 227 (2018) 123–132

Geochimica et Cosmochimica Acta

www.elsevier.com/locate/gca

More than ten million years of hyper-aridity recorded in the Atacama Gravels

Tao Sun [a,b,*], Huiming Bao [a], Martin Reich [c], Sidney R. Hemming [d]

[a] Geology and Geophysics Department, Louisiana State University, Baton Rouge, LA 70803, United States
[b] Astromaterial Research and Exploration Science Directorate, NASA Johnson Space Center, Houston, TX 77058, United States
[c] Department of Geology and Andean Geothermal Center of Excellence (CEGA), Universidad de Chile, FCFM, Santiago, Chile
[d] Department of Earth and Environmental Sciences and Lamont-Doherty Earth Observatory, Columbia University, Palisades, NY 10964, United States

Received 17 October 2017; accepted in revised form 11 February 2018; available online 21 February 2018

Abstract

The Atacama Desert's hyper-aridity is closely linked to the development of world-class copper and nitrate/iodine ores and to regional tectonics and global paleoclimate changes in the Cenozoic era. The timing when the hyper-aridity commenced remains controversial, with proposed ages ranging from Late Oligocene to Pleistocene. In this study, we provide an independent constraint on the initiation of Atacama hyper-aridity utilizing a 100-m deep profile within the Atacama Gravels and underneath porphyry copper deposit in Spence, northern Chile. The overall high concentration of sulfate (up to 10 wt%) and a multimodal distribution of water soluble salt (sulfates, chlorides and nitrates) indicate multiple generations of sedimentation and salt accumulation events under semi-arid to hyper-arid climate conditions. The multiple sulfate isotope compositions ($\Delta^{17}O$, $\delta^{18}O$, $\delta^{34}S$) of the upper section (−15.0 to −34.5 m) are close to those of modern hyperarid surface sulfates, while the lower section (−34.5 to −65 m) displays a depth dependent isotope trend that is best interpreted as marking a period of climate change from semi-arid to hyper-arid. When these data are combined with new chronological $^{40}Ar/^{39}Ar$ dates obtained from a volcanic ash layer at depth of −28.0 m, our results show that hyper-arid condition in the Atacama Desert was prevailing at least prior to 9.47 Ma and may go back as old as the middle Miocene.
© 2018 Elsevier Ltd. All rights reserved.

Keywords: Atacama; Hyperaridity; Sulfate; Triple oxygen isotopes

1. INTRODUCTION

The extreme climate in the Atacama Desert contributes to several unique features including the formation and preservation of massive nitrate/iodine deposits, the world's largest supergene Cu deposits containing the climate-sensitive mineral atacamite ($Cu_2Cl(OH)_3$), and the oldest landform with extremely low erosion rates. It has been argued that extremely arid climate could have played a role in the rise of the Andes (Lamb and Davis, 2003). Alternatively, paleoclimate observations from the southern Altiplano region (east of the study area) suggest that middle-late Miocene surface uplift of the Andean Plateau (Garzione et al., 2014) could have enhanced aridity of the western slope of the Andes. Knowing the timing, history, and cause(s) of the climatic transition from semi-aridity (>100 mm annual precipitation) to the current hyper-aridity (<10 mm annual precipitation) is therefore critical to understanding the global climate changes and their interplay with the tectonic evolution of South America, and to the exploration of mineral resources.

* Corresponding author at: Department of Earth Sciences, Rice University, United States.
E-mail address: tao.sun@rice.edu (T. Sun).

https://doi.org/10.1016/j.gca.2018.02.021
0016-7037/© 2018 Elsevier Ltd. All rights reserved.

The published estimated ages for the onset of present-day hyper-aridity range from Oligocene to Pleistocene (Alpers and Brimhall, 1988; Sillitoe and McKee, 1996; Hartley and Chong, 2002; Nishiizumi et al., 2005; Arancibia et al., 2006; Clarke, 2006; Rech et al., 2006; Reich et al., 2008; Amundson et al., 2012b). Most of these previous investigations have focused on climate-sensitive materials and/or processes including, the spatial distribution of evaporite deposits since Jurassic(Clarke, 2006; Hartley et al., 2005), the dependence of Cu supergene enrichment on water availability (Alpers and Brimhall, 1988; Sillitoe and McKee, 1996; Arancibia et al., 2006; Reich et al., 2008), cosmogenic nuclide accumulation in erosion-sensitive landforms (Dunai et al., 2005; Nishiizumi et al., 2005), drastic fluctuations in the sedimentological and geochemical properties of paleosols (Rech et al., 2006) and geomorphological and topographic changes in landscape features (Hartley and Chong, 2002; Amundson et al., 2012b). Despite these significant advances, the exact timing, and thus the primary trigger of transition into hyper-aridity remains controversial. This is partially, if not mainly, due to spatial climate heterogeneity, temporal climate oscillations, and sensitivities of aridity proxies in response to local tectonic/climatic/hydrological conditions as revealed from those studies. The main debate lies in whether the rain shadow effect associated with Andes rise during the Miocene or global cooling during the Pliocene-Pleistocene were the primary cause. In this study, we investigated the chemical and isotopic signatures of salts (notably sulfates) within a Miocene-age deep alluvial sedimentary sequence (Atacama Gravels, Atacama Gravel), focusing on a continuous archive that records critical climatic transitions in line with recent studies on paleosol development since the middle Miocene (e.g. (Clarke, 2006; Rech et al., 2006; Oerter et al., 2016)).

Due to the lack of groundwater movement near the surface, sulfate accumulations on today's hyper-arid surface of the Atacama Desert are mainly the result of atmospheric deposition, with contributions from seawater aerosol (near the coast), secondary atmospheric sulfate, and redistribution of Andean salt deposits via eolian processes (Ericksen, 1983; Berger and Cooke, 1997; Bao et al., 2004; Amundson et al., 2012a). Secondary atmospheric sulfate – i.e., sulfate formed via oxidation of sulfur gases from oceanic (dimethyl sulfide) volcanic (SO_2 and H_2S), and anthropogenic emissions by ozone (O_3), hydrogen peroxide (H_2O_2), metal-catalyzed O_2, and other oxidants in the atmosphere – is the only source of sulfate known to bear non-mass-dependent ^{17}O enrichment (where $\Delta^{17}O = \delta^{17}O - 0.52 * \delta^{18}O > 0$), in contrast to all other sulfate sources whose $\Delta^{17}O$ is at or slightly lower than 0 (Alexander et al., 2009; Bao, 2015; Bao et al., 2016). The accumulation of sulfates with positive $\Delta^{17}O$ values within surface regolith is a distinct feature of arid desert environments due mainly to the lack of post-depositional alteration by limitation of water (Michalski and Rech, 2004; Bao, 2005). The detection of sulfate $\Delta^{17}O$ values (>+0.2‰) within Atacama surface deposits thus is a good indication of a hyper-arid climatic state. Therefore, the preservation and pattern of sedimentary and mineralogical features, salt concentration and isotope composition such as $\delta^{17}O$, $\delta^{34}S$, and $\delta^{18}O$ profiles in the deep Atacama Gravel could reveal the desiccation history of the Atacama Desert, specifically the age for the onset of the hyper-aridity when combined with $^{40}Ar/^{39}Ar$ ages from a volcanic ash bed within the Atacama Gravel.

2. GEOLOGY CONTEXT AND SAMPLING SITE

A deep exploration drill core was obtained at Spence (22°47.3S, 69°15.3W, 1700 m a.b.s.l), a world-class porphyry copper deposit located in the east margin of the Central Depression, a longitudinal morphotectonic unit extending from marginal Pre-Cordillera to the eastern slope of the Coastal Cordillera, ~20 km west to the Domeyko fault zone (Fig. 1). Hypogene copper mineralization at Spence occurred during the Late Paleocene to Early Eocene, and the Cu deposit consists of a primary sulfide-bearing ore body overlaid by a secondary, ~200-m thick supergene Cu enrichment zone. The supergene Cu blanket contains atacamite ($Cu_2(Cl)(OH)_3$) and brochantite ($Cu_4(SO_4)(OH)_6$)) and was formed between 44.4 and 25.7 Ma (Cameron et al., 2007). The whole Cu deposit is covered by Atacama Gravel (Mortimer, 1973). The Neogene Atacama Gravel (average 150–200 m, up to ~600 m in thickness) was originally defined as poorly consolidated sedimentary deposits dominating the present landscape of the southern Atacama (south of ~26°S), and is now extending to the eastern flank of the Central Depression and some Pre-Cordillera basins (north to ~20°S) (Mortimer, 1973; Clarke, 2006; Nalpas et al., 2008; Jordan et al., 2010). Landforms in some northern and western flanks of the Central Depression are covered by Atacama Gravel of various ages, ranging from early Miocene to Pleistocene (Saez et al., 1999; Cameron et al., 2007). Generically, the Miocene Atacama Gravel are considered to be the integrated results of past climatic and tectonic changes (Riquelme et al., 2007; Nalpas et al., 2008). Its deposition likely occurred since the early Miocene by means of debris-flow and sheet flood from the Pre-Andean region down to the low elevation paleo-valleys that were previously formed under wetter conditions during the Oligocene (Riquelme et al., 2007). It was suggested that the sediment transport capacity was significantly reduced with increasing aridity, and deposition ceased at the initiation of hyper-aridity, around 9 to 5 Ma in the Central Depression (Nalpas et al., 2008). Therefore, the Miocene Atacama Gravel most likely record the end of a semi-arid to arid climate that provided episodic sediment depositions and the onset of a hyper-arid climate conditions that allowed the preservation of the Atacama Gravel and the salts therein.

The Atacama Gravel at Spence are composed of a 30–180 m thick sequence of presently indurated and impermeable gravels cemented by calcretes (Cameron et al., 2007). An unconformity separates the Atacama Gravel into two morphological distinct units similar to the nearby Atacama Gravel at El Tesoro (Tapia et al., 2011; Oerter et al., 2016), with upper (−15 to −34.5 m) and lower (−34.5 to −65 m) sections (Fig. 2). We took samples with 0.3 to 0.5 m sampling intervals from a drill core of the Atacama Gravel from depths of −15 m to −65 m, with 0 m marking the

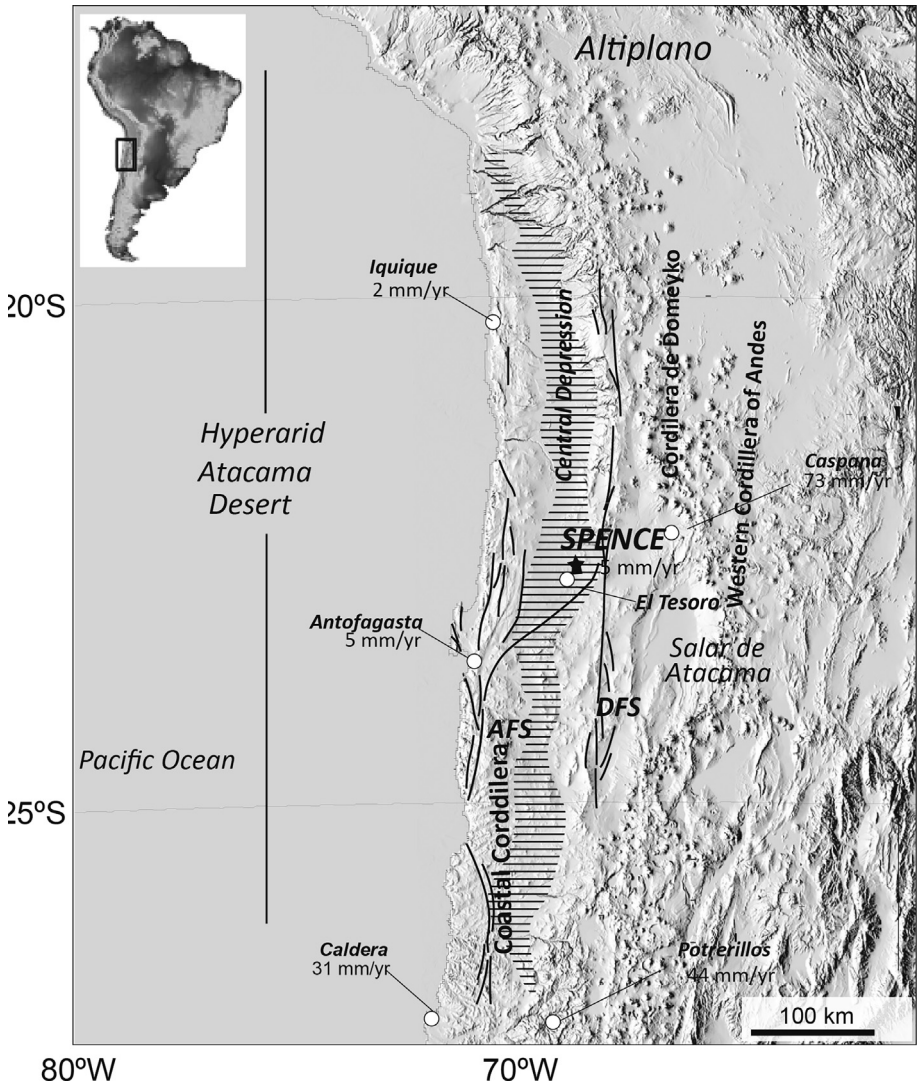

Fig. 1. Map of studied area of the Atacama Desert, northern Chile. Map shows four major geomorphological regions, West Andean Cordillera, Precordillera, Central Depression and Coastal Cordillera; and major structural features are also shown as the Atacama Fault System (AFS), the Antofagasta-Calama Lineament (ACL), and the Domeyko Fault System (DFS). Our sampling site is marked with square shape, annual average precipitation is also shown in comparison to other localities in the Atacama Desert.

surface. Center portion of the core samples were taken to avoid surface contamination from eolian processes. Shallow-depth samples were taken to a depth of −1.5 m near the drill site for reference (Fig. 2). In addition, gypsum samples intimately intergrown with atacamite were taken at the transition between the unlithified gravel cover and the underlying supergene Cu deposit at depths of −70 to −100 m. These were retrieved from a freshly exposed outcrop in the main mining pit, ~200 m laterally from the drill core site (Fig. 2). Mineralogical and chemical data of the Atacama Gravel and surface regolith were obtained. These data were coupled with isotopic measurements of $\Delta^{17}O$, $\delta^{18}O$ and $\delta^{34}S$ of sulfates within Atacama Gravel and supergene zone, together with two nitrate isotope data from the depths of −39 and −46 m. As a result, we produced a composite ~100-m vertical data profile. Furthermore, at a depth of ~−28 m, a volcanic ash layer (30–40 cm in thickness) was recognized in the drill core which is matched with a distinctive white-colored ash bed within the Atacama Gravel visible in the nearby mining pit. We conducted $^{40}Ar/^{39}Ar$ dating on grains including sanidine and plagioclase picked from this ash layer. No apparent paleosol development was observed for the sampled Atacama Gravel profile. Groundwater table was not observed in the >80-m deep mining pit.

3. METHODS

For each drill core samples and porphyry rock with intergrown gypsum, water-soluble ion was step-wised extracted using pH 2 HCl. The completeness of the dissolution and concentrations were determined/measured at Louisiana State University (LSU) using Ion Chromatography (Dionex ICS-3000). Mineralogy were determined using

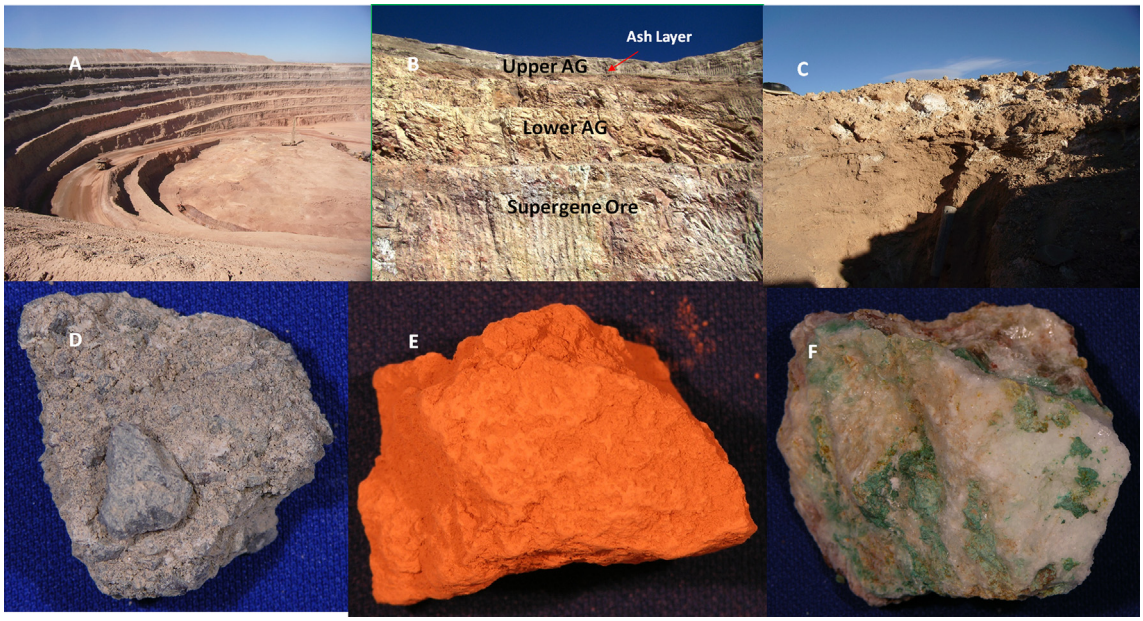

Fig. 2. Field photos of sampling site at Spence, north Chile and specimen. (A) Mining pit that is in ~200 m distance laterally from the drill core site; (B) A close look of the mining pit wall showing Atacama Gravel and supergene formations; (C) Shallow regolith where surface samples were collected; (D–F) show specimen of upper Atacama Gravel, lower Atacama Gravel and supergene atacamite/gypsum assemblage, respectively.

Panalytical X'Pert Pro MPD with X'celerator detector at the Johnson Space Center in Houston (Supporting Information). Note that, the drill core samples were crushed and well mixed prior to the salt extraction and XRD analysis. Sulfates were extracted as $BaSO_4$ for stable oxygen ($\Delta^{17}O$ and $\delta^{18}O$) and sulfur ($\delta^{34}S$) isotope measurement using Stable Isotope Ratio Mass Spectrometry (Thermo MAT-253 and Delta V, respectively) (Bao, 2006). Nitrates were extracted through cation exchange (CHG-10H resin) and subsequently precipitated as $AgNO_3$. Oxygen (O_2) was produced by thermo-decomposition of $AgNO_3$ at ~500 °C and $\Delta^{17}O$ was measured using MAT-253 (Michalski et al., 2002). All stable isotope analysis was conducted at LSU.

$^{40}Ar/^{39}Ar$ dating was performed at Lamont-Doherty Earth Observatory. Samples were co-irradiated with Alder Creek at the USGS TRIGA reactor in Denver and then analyzed by static peak hopping on a VG5400 noble gas mass spectrometer with analogue multiplier, after crystals were fused with a CO_2 laser and cleaned with ST 707 getters from SAES run at 2 amps. Data are corrected for blanks and mass discrimination based on frequent measurements of blanks and air pipettes and nuclear interferences based on published estimates (Dalrymple et al., 1981). An age of 1.193 Ma was used for the J-value calculation (Renne et al., 1998), and this yielded an age of 0.768 ± 0.005 Ma for 5 co-irradiated Bishop tuff crystals.

4. RESULTS

The upper section (−15 to −34.5 m) and surface regolith of the Atacama Gravel profile at Spence consist of poorly sorted, clast-supported conglomerates with angular to sub-angular ungraded gravels (diameter up to 10 cm) within a sandy matrix. The main mineral phases are quartz, plagioclase and anhydrite with minor amounts of mica. The lower section (−34.5 to −65 m) contains well-sorted, fine to coarse sands and silts where the dominant phases are quartz, clay minerals and gypsum (see Supporting Information). The concentration profiles of major water-soluble salts (SO_4^{2-}, Cl^-, NO_3^-) within the drill core show multimodal trends within the measured ~50 m (Fig. 3). SO_4^{2-} concentration co-varies with that of Ca^{2+} and displays a pronounced "zigzag" pattern; Both Cl^- and NO_3^- concentrations show two significant positive excursions at −17.2 and −39.0 m. The lowest concentrations for three anions all reside at the boundary between the upper and lower sections, i.e., at −34.5 m.

The sulfate isotope compositions in the upper section are in a narrow range of variation, with a weighted average of +8.3‰ for $\delta^{18}O$, +4.9‰ for $\delta^{34}S$, and +0.26‰ for $\Delta^{17}O$. These values are almost identical to those of sulfate in the surface regolith, which are +7.5‰, +4.2‰, and +0.27‰, respectively (Fig. 3). With increasing depth, the lower section exhibits increasing $\delta^{18}O$ (+6.8 to +10.2‰) and decreasing $\Delta^{17}O$ from +0.29 to −0.04‰, all in a narrow range of $\delta^{34}S$ with weighted average at +3.5‰. At the transition between the gravels and the supergene ore body (Fig. 3), gypsum shows distinctively different $\delta^{18}O$, $\delta^{34}S$ and $\Delta^{17}O$ values at +14.4 to +17‰, ~+4.3‰, and −0.04 to −0.20‰, respectively. The two nitrate samples from depth of −39 and −46 m show pronounced positive $\Delta^{17}O$ values at +15.1‰ and +10.3‰, respectively.

$^{40}Ar/^{39}Ar$ dating of three most radiogenic samples in the white volcanic tuff layer at −28 m give an age of 9.47 ± 0.04 Ma, m.s.w.d of 0.3 (Fig. 4).

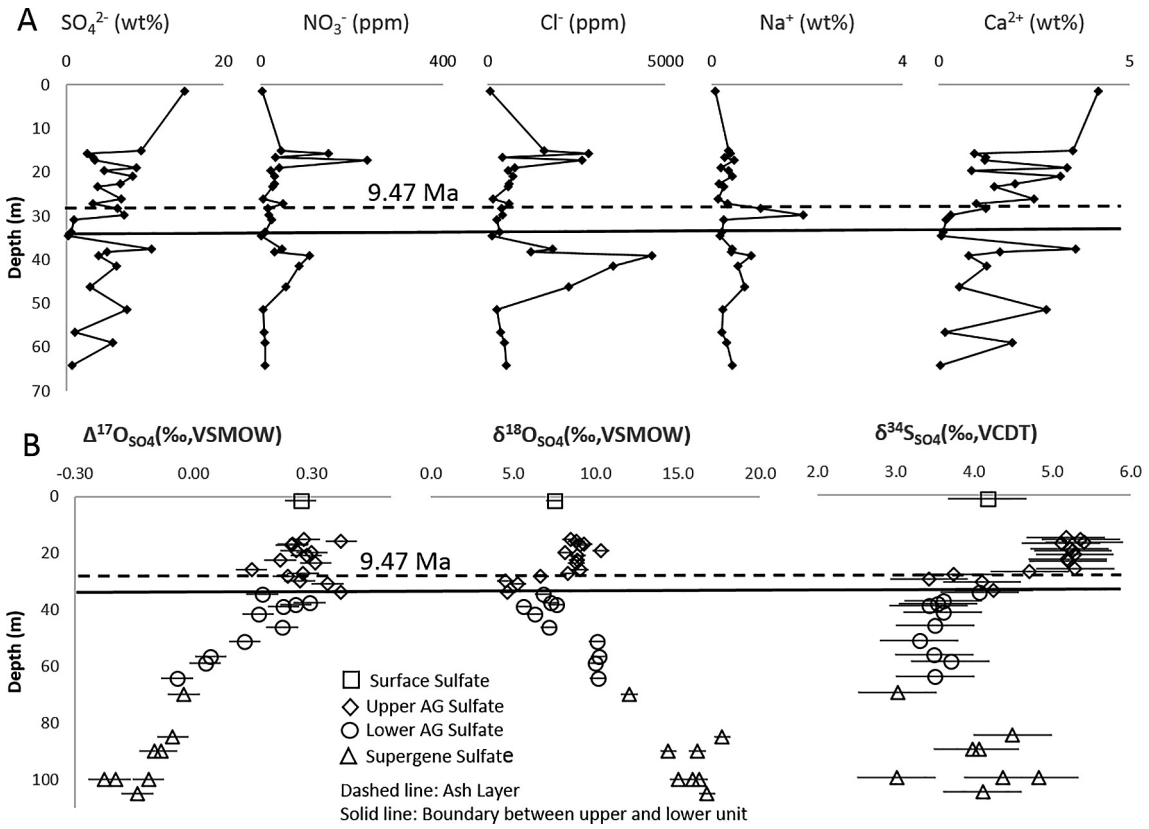

Fig. 3. (A): Major soluble anion (SO_4^{2-}, Cl^- and NO_3^-) weight concentration profiles from an Atacama Gravel drill core at Spence, northern Chile. Data show that their concentrations vary with depths. A surface regolith sample is included as reference of modern Atacama Gravel material. Dashed and solid lines reflect the positions of a volcanic ash layer at ~−28 m and the sedimentary boundary (between the upper and the lower sections) at ~−34 m, respectively. (B) Changing stable isotope compositions of sulfate ($\Delta^{17}O$, $\delta^{18}O$, $\delta^{34}S$) with depths. Data include a surface regolith sulfate, drill core sulfates and supergene sulfates from mining pit. Dashed and solid lines mark the positions of volcanic ash layer at ~−28 m and the sedimentary boundary (between the upper and the lower sections) at ~−34 m, respectively.

5. DISCUSSION

5.1. Atacama Gravel morphology and salt content indicating a hyper-arid climate prevailed after the deposition of the lower Atacama Gravel

The observed morphological and compositional differences of the lower and upper Atacama Gravel sections may be contributed to the variation in both climate and tectonic conditions which govern the sediment transport, deposition, and sediment source regions. The sedimentary facies in lower section are consistent with an overall dry, but relative wetter climate, deposited by low energy sheet flows with standing water at distal locations. The upper section sediments are largely deposited by sub-aerial high energy debris flow from proximal locations (Nalpas et al., 2008 and references therein). Although the relief between east margin of the Central Depression and that of the Pre-Cordillera probably has elevated since the early Miocene due partially to the regional monoclinal tilting, however, the studied region likely only experienced minor uplift (Jordan et al., 2010). Therefore, the source sediments of the alluvial fans may be largely attributed to climatic changes, rather than the tectonic changes.

The alluvial parent materials that fed the Central Depression are considered free of or at least low and homogeneous with depth in salt content. Salt additions were mostly derived from atmospheric deposition via airborne and eolian processes (Berger and Cooke, 1997; Bao et al., 2004; Clarke, 2006; Ewing et al., 2008; Amundson et al., 2012a). Compositional and isotopic variations of salts within alluvial fans thus vary with geographic/topographic locations due to source variability as well as post-depositional processes which are mainly controlled by the frequency and magnitude of wet events that infiltrated salts downward (i.e. top-down leaching) (Bao et al., 2004; Ewing et al., 2008; Amundson et al., 2012a) or occasional flash-flood or groundwater evaporation (i.e. bottom-up addition). The depth distribution of salt in a close-system soil profile in arid environment like Atacama is expected to be largely unimodal regardless of a top-down or a bottom-up process (Ewing et al., 2008; Amundson et al., 2012a). We argue that the observed multimodal pattern suggests that the deep Atacama Gravel profile at Spence is a composite profile generated from multi-episodes of Atacama Gravel deposition and subsequent salt accumulation. Post-depositional salt leaching (dissolution/precipitation) events appear to not have been frequent or massive enough to significantly

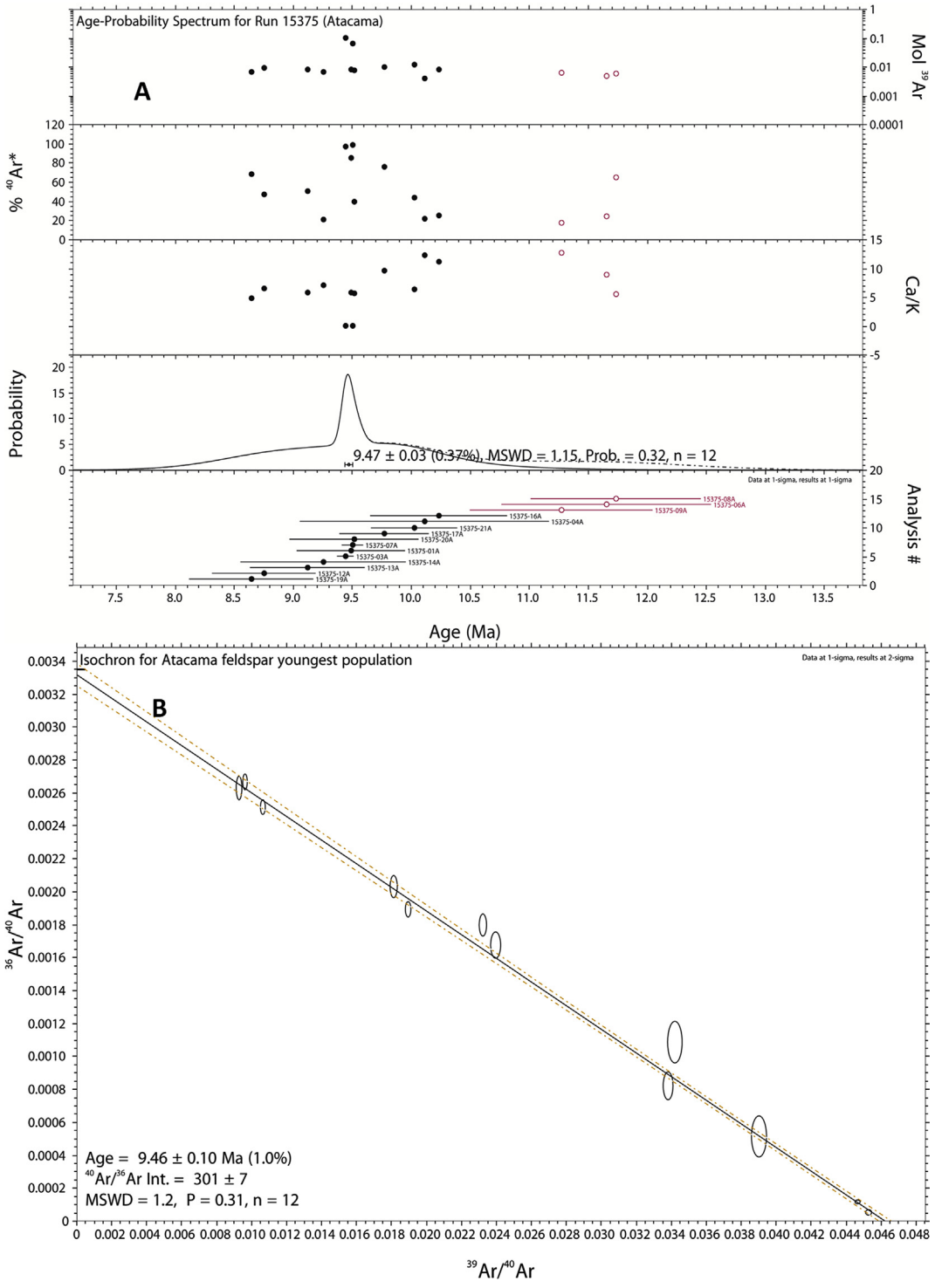

Fig. 4. (A) Probability plot. $^{40}Ar/^{39}Ar$ measurements were made on 21 individual grains picked from the density fraction $2.55 < D < 2.64$ extracted from a 20 to 100 cm thick, distinctly white volcanic tuff layer found intercalated within gravel deposits at depth of −28 m to provide the reported age estimate. Of the 21 grains, 15 yielded sufficient ^{39}Ar to calculate an age, and of those 15, 3 appear to be detrital, with ages >11 Ma. Two of the crystals have low Ca/K (most likely sanidine) and accordingly smaller errors, and those two crystals yield ages of 9.45 ± 0.04 and 9.51 ± 0.06 Ma. One plagioclase analysis also had %radiogenic >80% and yielded a similar age of 9.49 ± 0.44. Our best interpretation of the age is based on the 3 most radiogenic samples and is 9.47 ± 0.04, m.s.w.d of 0.3. (B) Isochron. All of the 12 grains with ages less than 11 Ma lie on an isochron with age of 9.46 ± 0.10, initial $^{40}Ar/^{36}Ar$ of 301 ± 7, and m.s.w.d of 1.2, suggesting that all come from the same population.

impact the sulfate concentrations of previously buried deposits. The salts could alternatively all be leached from the surface long after the cessation of the gravel deposition, and redistributed in the deep Atacama gravel profile. Such salts infiltration, however, requires environment with wet events of high frequency and large magnitude that would have left a relatively uniform and low salt profile (Fig. 3A). This scenario also requires substantial surface salt accumulations that is only favorable under arid/hyper-arid climate (Bao et al., 2004; Ewing et al., 2006), therefore is considered implausible. Interaction between the salt inventories of the upper and lower sections appears negligible based on the salt distribution pattern, specifically on the minimum concentration of all three anions at the unconformity. This indicates strongly that the salts accumulation within the lower Atacama Gravel section predate the upper Atacama Gravel deposition. Alternatively, the minimum salt concentrations might be result of salt profile being discontinued by subsurface ground water with flow path preferentially along the unconformity. The only subsurface water movement reported in this region was occasional highly saline formation water down within the supergene ore body (Cameron et al., 2007). Also, the paleosol preservation (Oerter et al., 2016) and absence of clay formation (Supporting Information) were observed near the unconformity. Therefore, we consider this possibility unlikely. All the observations are consistent with an overall arid to hyper-arid climate in this region after the deposition of lower Atacama Gravel section.

5.2. Multi-isotope profiles marking the lower Atacama Gravel section as the arid to hyper-arid transition

At Spence, surface deposition of sulfate includes secondary atmospheric sulfates and dusts. At greater depths where the supergene Cu ore body is present, sulfate minerals including alunite, jarosite and gypsum formed from supergene oxidation (Hartley and Rice, 2005). These sulfate sources have their characteristic set of stable isotope signatures (Bao, 2005; Bao and Marchant, 2006; Ewing et al., 2008; Amundson et al., 2012a). When examined in centimeter-scale, sulfate $\delta^{34}S$, $\delta^{18}O$, and $\Delta^{17}O$ values vary with depths from the surface. In McMurdo Dry Valleys of the Antarctica, this variation is interpreted as the result of preferential leaching one over the other between two different sulfate sources, i.e. SAS (H_2SO_4 and $(NH_4)_2SO_4$) and sea-salt (Na_2SO_4) initially deposited on soil surface. Calcium isotopes and sulfate sulfur and oxygen isotopes have been reported to vary as a function of depth in the Atacama, which was attributed to fractionation caused by meteoric water leaching and subsequent evaporation-driven re-precipitation and compounded by a Rayleigh process (Bao et al., 2004; Bao, 2005; Bao and Marchant, 2006; Ewing et al., 2008; Amundson et al., 2012a). The centimeter-scale isotope variations with depths may be present near the surface of Atacama Desert soils and these variations in deep sections could be re-worked by subsequent deposition, leaching, and re-precipitation of salts. The isotope variation shown in Fig. 3, however, is much larger in degree as well as in spatial scale. We argue that, to the first order, these salt isotope variations are consistent with concentration profiles, supporting episodic Atacama Gravel depositions and subsequent salt depositions and leaching from the surface during the sedimentary hiatuses.

The isotope compositions of sulfates in the upper section and surface regolith indicate that the formation pathways and source proportioning for the Atacama Gravel sulfates have remained constant since the deposition of the upper section. The surface and upper section sulfates all have $\Delta^{17}O$ values of $\sim$+0.25‰. For an average $\Delta^{17}O$ value of $\sim$ +0.70‰ for secondary atmospheric sulfates in mid-latitudes (Jenkins and Bao, 2006), secondary atmospheric sulfates then constitutes about $\sim$40% of the total surface sulfate deposition at Spence. Considering the fact that the $\delta^{34}S$ and $\delta^{18}O$ of bulk sulfate is close to a mixture of secondary atmospheric sulfates with the sulfate from Andean lakes, salars, and bed rock weathering from Altiplano (Bao et al., 2004; Clarke, 2006; Boschetti et al., 2007; Ewing et al., 2008), these multiple isotope signatures of surface sulfate are consistent with the present geographic and climatic setting of the region. We therefore conclude that the upper section of the Atacama Gravel profile at Spence is best interpreted by a series of small and relatively rapid debris depositions with intervals of hyper-aridity, during which atmospheric salts were deposited and later leached down into the gravel layer as a result of intermittent wetter events (Nester et al., 2007). The pronounced positive $\Delta^{17}O$ anomalies therefore support prevailing hyper-arid conditions during and after the deposition of the upper section gravels.

The sulfate $\Delta^{17}O$ in the upper $\sim$5 m of the lower section has the same positive values as those of the upper section, suggesting that a similarly hyper-arid climate condition has already been in place at the deposition of the upper lower section. This is also supported by the positive $\Delta^{17}O$ (+15.1‰ and +10.3‰) of nitrate samples from depth of −39 and −46 m, respectively (Michalski and Rech, 2004). On the other hand, the sulfate $\Delta^{17}O$ decrease with increasing depths from −41 to −65 m (Fig. 3B). Since secondary atmospheric sulfate is the sole source of the $\Delta^{17}O$-positive sulfate added into the Atacama Gravel profile, this trend may reflect a wetter climate during early stage of the lower Atacama Gravel deposition. Wetter climate (semi-arid) favored enhanced bed rock weathering and wet deposition of salts, subsequently the secondary atmospheric sulfate proportion in total atmospheric sulfate input was less than when under drier climate. Wetter climate also provide sufficient moisture to support microbial sulfate reprocessing within sediments which attenuated the positive $\Delta^{17}O$ signatures. The anticipated changes on $\delta^{34}S$ and $\delta^{18}O$ (Fig. 3B) by wetter climate may also support this scenario because (1) the salar or Andean sulfates possess very similar sulfur isotope compositions to the Spence surface sulfates (Rech et al., 2003) thus left negligible impact on the $\delta^{34}S$ and (2) sulfate redox cycles facilitated by microbes may elevate the $\delta^{18}O$ by involvement of evaporated meteoric water during this process.

An alternative scenario is that supergene deep sulfate was transported upward to mix with the lower Atacama Gravel sulfates, via groundwater capillary forcing or pumping induced by seismic events. The former only functions in a few meters' scale and the latter relies on fracture zones

(Hoke et al., 2004; Cameron et al., 2007; Perez-Fodich et al., 2014). Supergene sulfates seem to be one end member of this mixing. Sulfate formed via hypogene sulfide ore oxidation have a typical $\Delta^{17}O$ value as low as −0.20‰ (Bao et al., 2008), an anomalously high $\delta^{18}O$ indicative of involvement of saline groundwater that experienced intense evaporation ($\delta^{18}O_{H2O}$ as high as +10‰), in sharp contrast to that of the regional meteoric range at −8 to −11‰ (Cameron et al., 2007; Leybourne and Cameron, 2006). The $\delta^{34}S_{SO4}$ is also consistent with a sulfide source from the hypogene ore body of volcanic origin that normally ranges from ~−5 to +5‰. Because of the high salinity (Na-Cl type) of the local groundwater and deep formation water (Leybourne and Cameron, 2006), the mixing mechanism would have created a very high concentration of sodium and chloride in the lower section (Cameron et al., 2007), contradicting to our ion distribution profile. Thus, we conclude that this upward pumping and mixing scenario is less likely.

In addition, the $\Delta^{17}O$, $\delta^{18}O_{SO4}$ and $\delta^{34}S_{SO4}$ of the supergene sulfates values of supergene-ore related sulfate show a discernable trend from −0.05‰ to −0.20‰, +14.4 to +17.7 ‰ and +3.0 to +4.8‰, respectively, with increasing depths. This further indicates that the downward leaching and mixing of Atacama Gravel sulfate into the supergene sulfates, not the other way around. Therefore, we argue that most portion of the lower section of the Atacama Gravel profile at Spence likely reflects an overall arid climate condition with a transition from relatively wetter to hyper-arid.

5.3. Age of hyper-aridity

The sedimentological, salt concentration and isotope profiles of the deep Atacama Gravel section all point to the onset of a hyper-arid condition occurred since the deposition of the top part of the lower Atacama Gravel, which postdates the cessation of major supergene mobilization and mineralization at 21 Ma (Rowland and Clark, 2001). Here a further constraint is made available by the distinct white-colored ash bed occurring at the low part of the upper section. Our Ar-Ar dates suggest that by 9.47 Ma, hyper-arid conditions had already been in place (Fig. 4). The high sulfate concentrations below the ash bed, which is within the upper Atacama Gravel section, are comparable to, if not greater than, those found in the modern Atacama Desert surfaces. It was shown that long-term salt addition to the surface regolith resulted in soil volume expansion and high concentration of water soluble salts in the Atacama aided by an extremely low erosion rate (Ewing et al., 2006). An estimated 1 million years are required for regolith to accumulate a sulfate concentration to the magnitude seen below the ash bed in the upper section. Considering that sedimentary hiatuses are common especially in a hyper-arid climate, the gap of sedimentation between upper and lower Atacama Gravel could be as long as 1–2 million years in the Miocene (Saez et al., 2012). Therefore, the hyper-aridity of this region likely started as early as ~12 Myrs ago. This independent constraint is in agreement with recent landscape evolution from Pampa del Tamarugal and paleosol characteristics from Calama basin and nearby El Tesoro deposits (Jordan et al., 2014; Oerter et al., 2016).

6. CONCLUDING REMARKS

The transition from arid to hyper-arid climate conditions in the Atacama Desert is recorded in morphological, chemical, and multiple sulfate isotope data of a deep Atacama Gravel profile in the Central Depression. Our results show that hyper-arid conditions were certainly established before 9.47 Ma, and may have commenced at 12 Ma or earlier. This is the time when the Altiplano and pre-cordillera were experiencing protracted rise, a more than 2000 m elevation change during 16 to 9 Ma. The rise could have created an enhanced rain shadow effect that blocked moisture entry from the continental interior in the east to the Atacama (Garzione et al., 2014). During the same time, the Humboldt cold current off the west coast of South America was also strengthened due to the cold polar current linked to an expansion of Antarctic Ice Sheet (Amiot et al., 2008). This reinforced cold water upwelling further prevented precipitation along the coastal region of South America (Garreaud et al., 2010). A combination of these factors could have triggered the long-term Atacama hyper-aridity. It is relevant to note that our results provide an independent time constraint on the onset of hyper-aridity and long-term climate history in the heart of the Atacama Desert rather than constraints on climatic oscillations in some region of the Atacama Desert in the past (e.g., Amundson et al., 2012b). For example, paleosol formations at the nearby El Tesoro Cu mine reveal a remarkable period of oscillations between relatively moist to semi-arid and arid climates during the mid-Cenozoic (Oerter et al., 2016). We also recognize that spatially, the climate evolution of different areas in Atacama Desert may not have been synchronized (Alpers and Brimhall, 1988; Evenstar et al., 2009; Jordan et al., 2014). Nevertheless, with temporal coverage and spatial extent over the entire Central Depression, Atacama Gravel provides a rich record of the Atacama desiccation history.

ACKNOWLEDGEMENTS

T.S thanks Economic Development Assistantship by Board of Regents, Louisiana; and NASA Postdoctoral Fellowship Program. H.B thanks financial support provided by Petroleum Research Fund (48343-AC2) and NSF (EAR-1251824). M.R thanks funding provided by the MSI Initiative "Millennium Nucleus for Metal Tracing along Subduction (NC130065)". Additional support was provided by FONDECYT grants 1070736 and 1100014, and FONDAP project FONDAP project 15090013 "Centro de Excelencia en Geotermia de los Andes, CEGA". We thank Mario Sáez and BHP-Billiton for field assistance at Spence. We also thank three reviewers for their constructive comments.

APPENDIX A. SUPPLEMENTARY MATERIAL

Supplementary data associated with this article can be found, in the online version, at https://doi.org/10.1016/j.gca.2018.02.021.

REFERENCES

Alexander B., Park R. J., Jacob D. J. and Gong S. L. (2009) Transition metal-catalyzed oxidation of atmospheric sulfur: Global implications for the sulfur budget. *J. Geophys. Res. – Atmospheres* **114**.

Alpers C. N. and Brimhall G. H. (1988) Middle miocene climatic-change in the atacama desert, northern chile - evidence from supergene mineralization at La-Escondida. *Geol. Soc. America Bulletin* **100**, 1640–1656.

Amiot R., Gohlich U. B., Lecuyer C., de Muizon C., Cappetta H., Fourel F., Heran M. A. and Martineau F. (2008) Oxygen isotope compositions of phosphate from Middle Miocene-Early Pliocene marine vertebrates of Peru. *Palaeogeogr. Palaeoclimatol. Palaeoecol.* **264**, 85–92.

Amundson R., Barnes J. D., Ewing S., Heimsath A. and Chong G. (2012a) The stable isotope composition of halite and sulfate of hyperarid soils and its relation to aqueous transport. *Geochim. Cosmochim. Acta* **99**, 271–286.

Amundson R., Dietrich W., Bellugi D., Ewing S., Nishiizumi K., Chong G., Owen J., Finkel R., Heimsath A., Stewart B. and Caffee M. (2012b) Geomorphologic evidence for the late Pliocene onset of hyperaridity in the Atacama Desert. *Geol. Soc. America Bulletin* **124**, 1048–1070.

Arancibia G., Matthews S. J. and De Arce C. P. (2006) K-Ar and Ar-40/Ar-39 geochronology of supergene processes in the Atacama Desert, Northern Chile: tectonic and climatic relations. *J. Geol. Soc.* **163**, 107–118.

Bao H. M. (2005) Sulfate in modem playa settings and in ash beds in hyperarid deserts: implication for the origin of O-17-anomalous sulfate in an Oligocene ash bed. *Chem. Geol.* **214**, 127–134.

Bao H. M. (2006) Purifying barite for oxygen isotope measurement by dissolution and reprecipitation in a chelating solution. *Anal. Chem.* **78**, 304–309.

Bao H. (2015) Sulfate: A time capsule for Earth's O-2, O-3, and H2O. *Chem. Geol.* **395**, 108–118.

Bao H. M. and Marchant D. R. (2006) Quantifying sulfate components and their variations in soils of the McMurdo Dry Valleys Antarctica. *J. Geophys. Res. – Atmospheres* **111**.

Bao H. M., Jenkins K. A., Khachaturyan M. and Diaz G. C. (2004) Different sulfate sources and their post-depositional migration in Atacama soils. *Earth Planetary Sci. Lett.* **224**, 577–587.

Bao H., Barnes J. D., Sharp Z. D. and Marchant D. R. (2008) Two chloride sources in soils of the McMurdo Dry Valleys Antarctica. *J. Geophys. Res. – Atmospheres* **113**.

Bao H. M. Z., Cao X. B. and Hayles J. A. (2016). Triple oxygen isotopes: fundamental relationships and applications. In Annual Review of Earth and Planetary Sciences (eds. R. Jeanloz and K.H. Freeman), Vol. 44, pp. 463-492.

Berger I. A. and Cooke R. U. (1997) The origin and distribution of salts on alluvial fans in the Atacama Desert, northern Chile. *Earth Surf. Process. Landforms* **22**, 581–600.

Boschetti T., Cortecci G., Barbieri M. and Mussi M. (2007) New and past geochemical data on fresh to brine waters of the Salar de Atacama and Andean Altiplano, northern Chile. *Geofluids* **7**, 33–50.

Cameron E. M., Leybourne M. I. and Palacios C. (2007) Atacamite in the oxide zone of copper deposits in northern Chile: involvement of deep formation waters? *Mineralium Deposita* **42**, 205–218.

Clarke J. D. A. (2006) Antiquity of aridity in the Chilean Atacama Desert. *Geomorphology* **73**, 101–114.

Dalrymple G. B., Alexander, Jr., E. C., Lanphere M. A. and Kraker G. P. (1981). Irradiation of Samples for 40Ar/39Ar Dating Using the Geological Survey TRIGA Reactor. In Geological Survey Professional Paper United States Government Printing Office (ed. U.S.G. Survey).

Dunai T. J., Lopez G. A. G. and Juez-Larre J. (2005) Oligocene-Miocene age of aridity in the Atacama Desert revealed by exposure dating of erosion-sensitive landforms. *Geology* **33**, 321–324.

Ericksen G. E. (1983) The Chilean nitrate deposits. *Am. Scientist* **71**, 366–374.

Evenstar L. A., Hartley A. J., Stuart F. M., Mather A. E., Rice C. M. and Chong G. (2009) Multiphase development of the Atacama Planation Surface recorded by cosmogenic (3)He exposure ages: implications for uplift and Cenozoic climate change in western South America. *Geology* **37**, 27–30.

Ewing S. A., Sutter B., Owen J., Nishiizumi K., Sharp W., Cliff S. S., Perry K., Dietrich W., McKay C. P. and Amundson R. (2006) A threshold in soil formation at Earth's arid-hyperarid transition. *Geochim. Cosmochim. Acta* **70**, 5293–5322.

Ewing S. A., Yang W., DePaolo D. J., Michalski G., Kendall C., Stewart B. W., Thiemens M. and Amundson R. (2008) Non-biological fractionation of stable Ca isotopes in soils of the Atacama Desert, Chile. *Geochim. Cosmochim. Acta* **72**, 1096–1110.

Garreaud R. D., Molina A. and Farias M. (2010) Andean uplift, ocean cooling and Atacama hyperaridity: a climate modeling perspective. *Earth Planetary Sci. Lett.* **292**, 39–50.

Garzione C. N., Auerbach D. J., Smith J. J. S., Rosario J. J., Passey B. H., Jordan T. E. and Eiler J. M. (2014) Clumped isotope evidence for diachronous surface cooling of the Altiplano and pulsed surface uplift of the Central Andes. *Earth Planetary Sci. Lett.* **393**, 173–181.

Hartley A. J. and Chong G. (2002) Late Pliocene age for the Atacama Desert: implications for the desertification of western South America. *Geology* **30**, 43–46.

Hartley A. J. and Rice C. M. (2005) Controls on supergene enrichment of porphyry copper deposits in the Central Andes: a review and discussion. *Mineralium Deposita* **40**, 515–525.

Hartley A. J., Chong G., Houston J. and Mather A. E. (2005) 150 million years of climatic stability: evidence from the Atacama Desert, northern Chile. *J. Geol. Soc.* **162**, 421–424.

Hoke G. D., Isacks B. L., Jordan T. E. and Yu J. S. (2004) Groundwater-sapping origin for the giant quebradas of northern Chile. *Geology* **32**, 605–608.

Jenkins K. A. and Bao H. (2006) Multiple oxygen and sulfur isotope compositions of atmospheric sulfate in Baton Rouge, LA, USA. *Atmospheric Environ.* **40**, 4528–4537.

Jordan T. E., Nester P. L., Blanco N., Hoke G. D., Davila F. and Tomlinson A. J. (2010) Uplift of the Altiplano-Puna plateau: a view from the west. *Tectonics* **29**.

Jordan T. E., Kirk-Lawlor N. E., Blanco N., Rech J. A. and Cosentino N. J. (2014) Landscape modification in response to repeated onset of hyperarid paleoclimate states since 14 Ma, Atacama Desert, Chile. *Geol. Soc. America Bulletin* **126**, 1016–1046.

Lamb S. and Davis P. (2003) Cenozoic climate change as a possible cause for the rise of the Andes. *Nature* **425**, 792–797.

Leybourne M. I. and Cameron E. M. (2006) Composition of groundwaters associated with porphyry-Cu deposits, Atacama Desert, Chile: Elemental and isotopic constraints on water sources and water-rock reactions. *Geochim. Cosmochim. Acta* **70**, 1616–1635.

Michalski G., Savarino J., Bohlke J. K. and Thiemens M. (2002) Determination of the total oxygen isotopic composition of nitrate and the calibration of a Delta O-17 nitrate reference material. *Anal. Chem.* **74**, 4989–4993.

Michalski G. and Rech J. (2004) Nitrate Delta O-17: Insights into the onset of hyperaridity in the atacama desert. *Abstracts Papers Am. Chem. Soc.* **228**, U699-U699.

Mortimer (1973) The Cenozoic history of the southern Atacama Desert. *J. Geol. Soc. Lond* **129**.

Nalpas T., Dabard M. P., Ruffet G., Vernon A., Mpodozis C., Loi A. and Herail G. (2008) Sedimentation and preservation of the Miocene Atacama Gravels in the Pedernales-Chanaral Area, Northern Chile: Climatic or tectonic control? *Tectonophysics* **459**, 161–173.

Nester P. L., Gayo E., Latorre C., Jordan T. E. and Blanco N. (2007) Perennial stream discharge in the hyperarid Atacama Desert of northern Chile during the latest Pleistocene. *Proc. Natl. Acad. Sci. USA* **104**, 19724–19729.

Nishiizumi K., Caffee M. W., Finkel R. C., Brimhall G. and Mote T. (2005) Remnants of a fossil alluvial fan landscape of Miocene age in the Atacama Desert of northern Chile using cosmogenic nuclide exposure age dating. *Earth Planetary Sci. Lett.* **237**, 499–507.

Oerter E., Amundson R., Heimsath A., Jungers M., Chong G. and Renne P. (2016) Early to middle miocene climate in the atacama desert of Northern Chile. *Palaeogeogr. Palaeoclimatol. Palaeoecol.* **441**, 890–900.

Perez-Fodich A., Reich M., Alvarez F., Snyder G. T., Schoenberg R., Vargas G., Muramatsu Y. and Fehn U. (2014) Climate change and tectonic uplift triggered the formation of the Atacama Desert's giant nitrate deposits. *Geology* **42**, 251–254.

Rech J. A., Quade J. and Hart W. S. (2003) Isotopic evidence for the source of Ca and S in soil gypsum, anhydrite and calcite in the Atacama Desert, Chile. *Geochim. Cosmochim. Acta* **67**, 575–586.

Rech J. A., Currie B. S., Michalski G. and Cowan A. M. (2006) Neogene climate change and uplift in the Atacama Desert, Chile. *Geology* **34**, 761–764.

Reich M., Palacios C., Parada M. A., Fehn U., Cameron E. M., Leybourne M. I. and Zuniga A. (2008) Atacamite formation by deep saline waters in copper deposits from the Atacama Desert, Chile: evidence from fluid inclusions, groundwater geochemistry, TEM, and (36)Cl data. *Mineralium Deposita* **43**, 663–675.

Renne P. R., Swisher C. C., Deino A. L., Karner D. B., Owens T. L. and DePaolo D. J. (1998) Intercalibration of standards, absolute ages and uncertainties in Ar-40/Ar-39 dating. *Chem. Geol.* **145**, 117–152.

Riquelme R., Herail G., Martinod J., Charrier R. and Darrozes J. (2007) Late Cenozoic geomorphologic signal of Andean forearc deformation and tilting associated with the uplift and climate changes of the Southern Atacama Desert (26 degrees S-28 degrees S). *Geomorphology* **86**, 283–306.

Rowland M. G. and Clark A. H., 2001. Temporal overlap of supergene alteration and high-sulfidation mineralization in the Spence porphyry copper deposit, II region, Chile. Geol. Soc. America, Abstracts Programs, 33, 538.

Saez A., Cabrera L., Jensen A. and Chong G. (1999) Late Neogene lacustrine record and palaeogeography in the Quillagua-Llamara basin, Central Andean fore-arc (northern Chile). *Palaeogeogr. Palaeoclimatol. Palaeoecol.* **151**, 5–37.

Saez A., Cabrera L., Garces M., van den Bogaard P., Jensen A. and Gimeno D. (2012) The stratigraphic record of changing hyperaridity in the Atacama desert over the last 10 Ma. *Earth Planet. Sci. Lett.* **355**, 32–38.

Sillitoe R. H. and McKee E. H. (1996) Age of supergene oxidation and enrichment in the Chilean porphyry copper province. *Econ. Geol. Bulletin Soc. Econ. Geol.* **91**, 164–179.

Tapia M., Riquelme R., Campos E., Marquardt C., Mpodozis S., Mora R., Munchmeyer, C., 2011. Cenozoic exotic Cu mineralization in the Centinela District (Atacama Desert, north Chile), Society of Geology Applied to Mineral Deposits, Antofagast, Chila.

Associate Editor: Miryam Bar-Matthews